NMR and ESCA Chemical Shifts in Aluminosilicates: A Critical Discussion

JACEK KLINOWSKI[*,†] AND TERY L. BARR[‡]

Department of Chemistry, University of Cambridge, Lensfield Road, Cambridge CB2 1EW, U.K., and Department of Materials and Laboratory for Surface Studies, University of Wisconsin—Milwaukee, Milwaukee, Wisconsin 53201

Received June 4, 1998

Introduction

The effect known as the chemical shift is central to the application of nuclear magnetic resonance (NMR) and electron spectroscopy for chemical analysis (ESCA) in the study of solids. While other techniques can also provide insights into structure, only ESCA and NMR give information which is directly relevant to chemical bonding, can

Jacek Klinowski has doctorates from the Jagiellonian University and from the University of London, and is a Master of Arts of the University of Cambridge, where he is Reader in Chemical Physics. He has over 360 publications and is Editor-in-Chief of *Solid-State Nuclear Magnetic Resonance*, an international journal. He is the coauthor of *Fundamentals of Nuclear Magnetic Resonance* (Longman, 1993) and of *A Primer of Magnetic Resonance Imaging* (Imperial College Press, 1998). He is a Foreign Member of the Polish Academy of Arts and Sciences, an Honorary Member of the Polish Chemical Society, and a Presidential Professor, Republic of Poland. His interests include solid-state NMR and ESCA study of micro- and mesoporous molecular sieves, minerals, ceramics, fullerenes, and biological samples.

Tery L. Barr, a Professor of Materials and Surface Studies at the University of Wisconsin—Milwaukee, received his B.S. in chemistry from the University of Virginia, M.S. from the University of South Carolina, and Ph.D. from the University of Oregon. Following postdoctoral work at the University of Washington, he held several faculty positions, including a visiting one at the University of California, Berkeley. He then became interested in ESCA, discovering the chemical shift in silicates and related inorganic materials. T. L. Barr was a Visiting Professor at the University of Uppsala (with Kai Siegbahn) and a Fulbright Visiting Professor at the University of Cambridge, where his collaboration with Jacek Klinowski began. He has over 150 publications and is the most often cited member of his faculty.

be obtained rapidly for almost any crystalline or amorphous solid, and is readily interpretable in structural terms. ESCA and NMR can now be used in tandem to address problems in catalysis, ceramics, and device technology: ESCA provides information concerning the surface (to a depth of ca. 50–100 Å), and NMR monitors the bulk of the material.

Although there is evidence that ESCA is insensitive to the outermost 5 Å of many solids,[1,2] it detects features which are not detected by NMR and vice versa, which is of critical importance to sorption and catalysis.[3,4] We shall discuss the optimization of the ESCA/NMR combination and the strengths and limitations of each technique. This is conveniently done using framework silicates, for which a substantial amount of data are available. The details of the measurements, acquired to the best level of precision and accuracy, can be found in the original papers cited.

Chemical Shift in NMR

The chemical shift is the basis of the application of NMR in chemistry. The electrons surrounding a magnetic nucleus interact with the static magnetic field, B_o, and the resulting secondary local magnetic field opposes B_o, thus "shielding" the nucleus from its full effect. The effect is anisotropic, which is described by the shielding Hamiltonian

$$H_{CS} = -\gamma \hbar \mathbf{I} \cdot \sigma \cdot \mathbf{B}_o \qquad (1)$$

where σ is a second-rank tensor ("the chemical shielding tensor"), axially symmetric in strong magnetic fields.[5] In the principal reference system (PAS) σ is decribed by three principal components, σ_{ii} ($i = 1, 2, 3$), and three direction cosines, $\cos \theta_i$, between the axes of PAS and the laboratory reference system.

The observed shielding constant, σ_{zz}, is a linear combination of the principal components

* To whom correspondence should be addressed. Phone: +(44)-1223-33 65 14. Fax: +(44)-1223-33 63 62. E-mail: jk18@cam.ac.uk.
† University of Cambridge.
‡ University of Wisconsin—Milwaukee.

$$\sigma_{zz} = \sum_{i=1}^{3} \sigma_{ii} \cos^2 \theta_i = \frac{1}{3} \operatorname{Tr} \sigma + \frac{1}{3}\sum_{i=1}^{3}(3 \cos^2 \theta_i - 1)\sigma_{ii}$$

$$(2)$$

where $\operatorname{Tr} \sigma$ stands for the trace of the tensor. Since the average value of each $\cos^2 \theta_i$ is 1/3, the average value of σ_{zz} in the NMR spectra of liquids (where there is random molecular tumbling) is the isotropic value

$$\overline{\sigma_{zz}} = \frac{1}{3} \operatorname{Tr} \sigma = \sigma_{iso} \qquad (3)$$

In solids the angle-dependent second term on the right of (3) survives, giving rise to a spread of resonance frequencies. In microcrystalline powders this results in a "powder pattern" which can be directly interpreted provided that dipolar and quadrupolar interactions are small. Magic-angle spinning (MAS) averages the chemical shift tensor to the isotropic chemical shift, quantified by comparing the resonance angular frequency, ω, with a specific resonance, ω_{ref}, in a reference compound.

Aluminosilicate frameworks are composed of silicon, aluminum, and oxygen. The extraframework charge-balancing cation is typically Na^+. Some properties of the nuclei which can be measured by NMR in aluminosilicates are listed in Table 1.

Chemical Shift in ESCA

The chemical shift in ESCA is defined[2] as the difference in binding energy, ΔE_J^A, of a core level J when the atom A is transferred from environment 1 to environment 2 (Figure 1).

$$\Delta E_J^A(1{\Rightarrow}2) = E_J^A(2) - E_J^A(1) \qquad (4)$$

Rigorous quantum mechanical calculation of core-level orbital energies $E_J^A(k)$ and many-body effects is avoided by using one of several approximations. The most useful is the charge potential model[6] in which

$$\Delta E_J^A(1{\Rightarrow}2) \approx \langle V_J \rangle^A \Delta Q^A(1{\Rightarrow}2) + \sum_{C \neq A}\left[\left(\frac{Q^C}{r_{AC}}\right)_2 - \left(\frac{Q^C}{r_{AC}}\right)_1\right] + L'$$

$$(5)$$

where Q^A and Q^C are the charges of atoms A and C, $\langle V_J \rangle^A$ is the average field interaction between a core electron and a valence electron on atom A, r_{AC} is the separation of atoms A and C, and L' fixes the scale for the problem. Sometimes state 1 is itself a common reference, such as the elemental state of A in the gas phase. The effects of state 1 may then be included in L' to give

$$\Delta E_J^A(1{\Rightarrow}2) = k^A \Delta Q^A(1{\Rightarrow}2) + \sum_{C \neq A}\left[\left(\frac{Q^C}{r_{AC}}\right)_2 - \left(\frac{Q^C}{r_{AC}}\right)_1\right] + L$$

$$(6)$$

where we assume that $k^A = \langle V_J \rangle^A$ is the same for all core-level states of atom A.

The *measured* ESCA chemical shift, ΔE_J^{mA}, is defined as the change in peak position of a core-level line when the chemical status of the atom is changed. When a metal

Table 1. NMR Properties of the Nuclei in Aluminosilicates

nucleus	spin I	natural abundance of C (%)	receptivity relative to ^{1}H (D)	quadrupole moment[a] $(10^{28}\ Q/m^2)$
^{17}O	5/2	3.7×10^{-2}	1.08×10^{-5}	-2.58×10^2
^{23}Na	3/2	100	9.27×10^{-2}	0.102
^{27}Al	5/2	100	0.207	0.149
^{29}Si	1/2	4.69	3.69×10^{-4}	

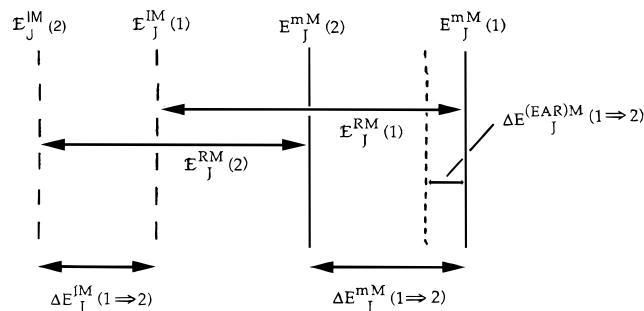[a] Defined as $D = |\gamma^3|CI(I+1)$ and normalized to $D_H = 1$.

FIGURE 1. ESCA chemical shift for the J electron of element M upon transition from species 1 (such as elemental metal M^o) to species 2 (such as oxide M_xO_y). The superscript I refers to the premeasurement initial state, and the superscript m to the measured final state. The final states are shifted from the initial states by the relaxation R. The chemical dependence of this relaxation is contained in the extra-atomic relaxation term, $\Delta E_J^{(EAR)}$. This is usually small and disappears when similar oxides are compared, so that $\Delta E_J^{mM}(1{\Rightarrow}2) \approx \Delta E_J^{IM}(1{\Rightarrow}2)$.

is oxidized from its elemental state, M^o, to the oxide

$$xM^o + y\frac{1}{2}O_2 \Rightarrow M_xO_y \qquad (7)$$

we have

$$\Delta E_J^{mM}(1{\Rightarrow}2) = E_J^{mM}(2) - E_J^{mM}(1) \qquad (8)$$

where (2) denotes the core state J of atom M in the oxide and (1) that in the elemental state. The measured energy $E_J^{mM}(i)$ may be approximated in terms of the orbital energy of core state J in the chemical condition i.

$$E_J^{mM}(i) \approx -E_J^M(i) \qquad (9)$$

This approximation neglects many-body effects and the fact that the measurement process itself alters the state of the material, so that atomic relaxation occurs before the result is recorded. A more correct form of (9) is therefore

$$E_J^{mM}(i) \approx E_J^{IM}(i) - E_J^{RM}(i) \qquad (10)$$

where E_J^{IM} is the energy of the initial (premeasurement) state of atom M and E_J^{RM} is the relaxation energy. Two problems arise: (1) chemical information is contained in E_J^{IM}, and (2) relaxation creates a complex hole−ion final state system, a rigorous description of which requires formidable quantum mechanical formulation which can be solved analytically only for simple systems.

These two problems may seem less severe when we are interested in the *change* of chemical state, and it might

Table 2. ESCA Binding Energies Referenced to C(1s), 284.6 eV, and, in Parentheses, Corresponding Line Widths ($\pm$0.05 eV) for Some Aluminosilicates

material	Si/Al	Si(2p)	Al(2p)	O(1s)
γ-Al$_2$O$_3$	0		73.80 (2.1)	530.55 (2.0)
zeolite Na-A	1.00	101.1 (1.7)	73.5 (1.6)	530.5 (1.75)
sodalite	1.05	101.5 (2.2)	73.5 (1.75)	530.9 (2.45)
zeolite Na-X	1.25	101.95 (1.75)	73.90 (1.6)	531.05 (1.65)
zeolite Na-Y	2.50	102.55 (1.7)	74.20 (1.55)	531.75 (2.05)
zeolite ZSM-5	>30	103.1 (1.8)	74.48 (1.8)	532.45 (1.95)
α-SiO$_2$	∞	103.55 (1.8)		532.85 (1.9)

appear that the contributions $\Delta E_J^{RM}(1{\Rightarrow}2)$ to the relaxation will cancel. Unfortunately, while $\Delta E_J^{RM}(1{\Rightarrow}2)$ is often small, the so-called extra-atomic relaxation (EAR)[7] is generally significant.

$$\Delta E_J^{mM}(1{\Rightarrow}2) = \Delta E_J^{IM}(1{\Rightarrow}2) - \Delta E_J^{(EAR)M}(1{\Rightarrow}2) \quad (11)$$

The differences in EAR are small and show a progression which maps a similar change of the shifts in the initial state, thus shifting ΔE^{IM} by small fixed amounts, which does not affect chemical arguments. For such systems the change in the measured binding energies may be interpreted directly in chemical terms. In closely related oxides such as SiO$_2$ and Al$_2$O$_3$, relaxation can be ignored without affecting the relationship between measured ESCA peak shifts and changes in chemistry.[8,9] The differences in relaxation effects between an elemental metal M and its oxides M$_x$O$_y$ are removed when dealing with two different oxides of M, because to first-order we are comparing different states of the same oxide ion.

NMR and ESCA Chemical Shifts in Aluminosilicates

NMR and ESCA chemical shifts for the elements found in aluminosilicates (Tables 1 and 2) lead to similar conclusions.[1–4,10–15] Differences arise in the surface-versus-bulk effects: ESCA shows that in catalysts made by mixing zeolites with alumina or clay the binder coats the catalyst particles with a layer ca. 100–200 Å thick. The subsurface component is often not detected by ESCA, while NMR can monitor the status of the zeolite before and after binding.

The most useful feature of ESCA and NMR is their sensitivity to the change in bonding when the structure or the aluminum content is altered. ^{29}Si NMR shifts[5] and Si(2s) and Si(2p) ESCA shifts[1,2,4,16] change progressively as the Si/Al ratio increases from Si/Al = 1.0 (zeolite Na-A) to Si/Al > 30 (ZSM-5). Similarly, ^{27}Al NMR[5] and Al(2s) or Al(2p) ESCA[1,2,4,16] chemical shifts for 4- and 6-coordinate aluminum are different. ESCA permits direct interpretation of its results in terms of the type of bonding, because it responds directly to charge densities at all atomic centers (eq 8).[1,2,17–19] For example, it shows that the Al–O bond in zeolite Na-Y is more ionic than in zeolite Na-X.[1,2,4,12,14–16]

Elemental NMR and ESCA Chemical Shifts

Silicon. The range of ^{29}Si chemical shifts in silicates is ca. 60 ppm.[5] High-resolution ^{29}Si NMR has established the
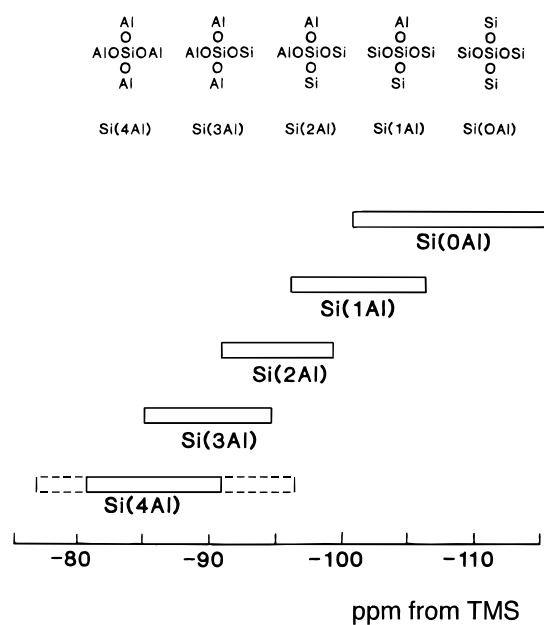

FIGURE 2. Ranges of ^{29}Si chemical shift for Si(nAl) building blocks in zeolites. The dotted line marks the exceptionally wide (from -76.5 to -97 ppm) range of chemical shifts for Si(4Al) in synthetic sodalites containing various enclathrated salts.[28]

structure of soluble silicate anions. The description of building units in silicates uses the "Q^n notation",[5,20] where Q stands for a silicon atom bonded to four oxygen atoms, forming a SiO$_4$ tetrahedron. The superscript n indicates the connectivity, i.e., the number of other Q units attached to the unit in question. The total range of chemical shifts from -60 to -120 ppm from tetramethylsilane (TMS) is split into intervals corresponding to monosilicates (Q^0), disilicates and chain end groups (Q^1), middle groups in chains (Q^2), chain branching sites (Q^3), and fully cross-linked framework sites (Q^4). In solids containing more than one type of Q^n unit, separate lines are observed.

As framework aluminosilicates also contain aluminate tetrahedra, the Q^n notation is insufficient. While the environment of each Si atom in framework silicates is always Q^4 (4Si), in aluminosilicates there are five Q^4 [nAl, $(4 - n)$Si] possibilities with $n = 0$, 1, 2, 3, or 4. We shall denote these as Si(nAl) or Si[$(4 - n)$Si], where n ($\leq$4) is the number of aluminum atoms connected, via oxygens, to a silicon. The replacement of one or more Si atoms in a Q^4 unit by Al atoms causes a significant paramagnetic shift: the substitution Si[$(n - 1)$Al] $\rightarrow$ Si(nAl) makes the ^{29}Si chemical shift less negative by ca. 5 ppm.

The ranges of ^{29}Si chemical shifts for the various Si-(nAl) building blocks in zeolites are shown in Figure 2. When Si/Al = 1.0, each Si atom is surrounded by four Al atoms and the spectrum is composed of a single Si(4Al) peak. For Si/Al > 1 there are five possibilities for the distribution of Al in the first tetrahedral shell: the lower aluminum content and the Loewenstein rule,[21] which prohibits Al–O–Al linkages, increase the populations of Si(3Al), Si(2Al), Si(1Al), and Si(0Al) at the expense of Si-(4Al). The ^{29}Si NMR spectra are primarily sensitive to the composition of the first tetrahedral coordination shell around each Si atom (Figure 3).
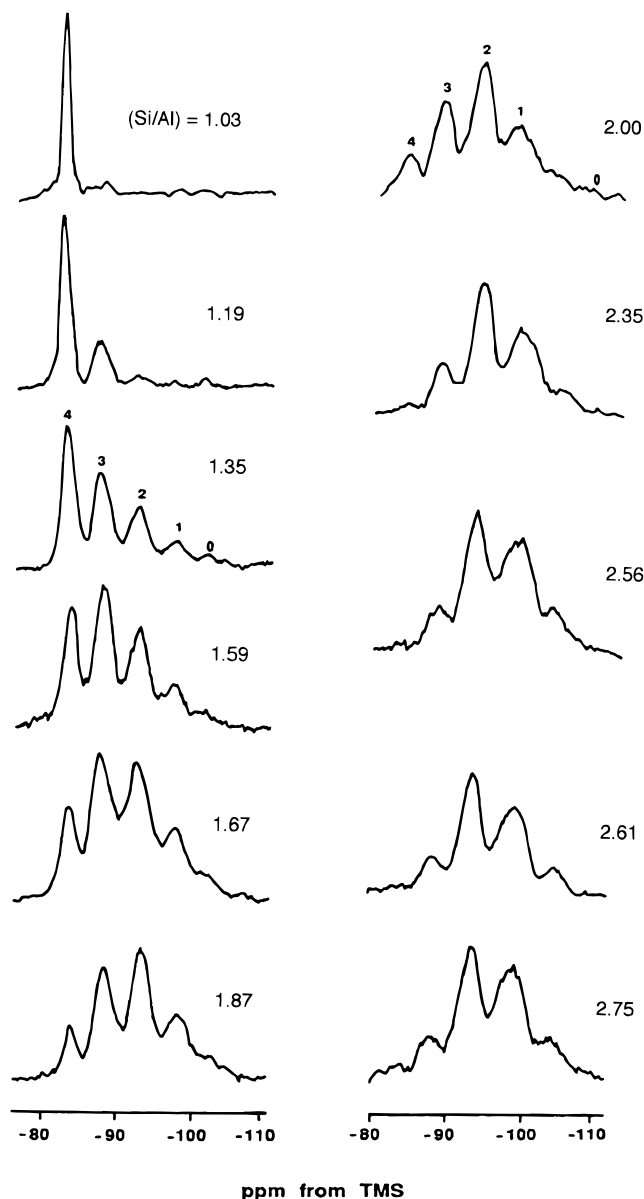
FIGURE 3. High-resolution ^{29}Si MAS NMR spectra of zeolites Na-X and Na-Y. Si(nAl) peaks are identified by the n above the peaks.

The Si/Al ratio in the zeolitic framework may be calculated from the ^{29}Si MAS NMR spectrum using the formula[5]

$$(\text{Si/Al})_{\text{NMR}} = \frac{I_4 + I_3 + I_2 + I_1 + I_0}{I_4 + 0.75I_3 + 0.5I_2 + 0.25I_1} \quad (12)$$

where I_n denotes the intensity of the NMR peak corresponding to the Si(nAl) unit.

^{29}Si NMR can be used to determine the *ordering* of Si and Al atoms in the framework.[20,22,23] Provided that the Si(nAl) units from crystallographically inequivalent Si atoms do not overlap, the areas under the spectral peaks are directly proportional to the populations of the respective structural units in the sample. These can be calculated from the spectrum (see Figure 3) and compared with the relative numbers of such units contained in models involving different Si, Al ordering schemes. A choice
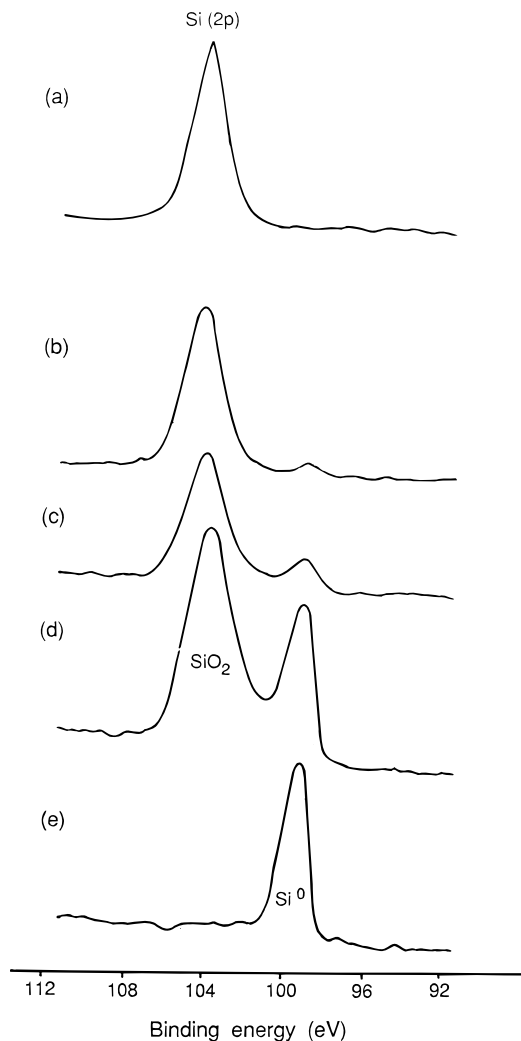
FIGURE 4. Si(2p) ESCA chemical shift. (a) The spectrum of a slab of silicon coated with a thin (but thicker than ca. 100 Å) layer of SiO$_2$ contains only the peak with the chemical shift of 103.25 eV, typical of SiO$_2$. (b) As the layer of silica is etched away with A$^+$ ions to a thickness of less than ca. 75 Å, the peak from elemental Si appears at 99.6 eV. (c) As the etching continues, the peak from elemental Si increases in intensity at the expense of the peak from SiO$_2$. (d) Finally, when all silica has been removed, only the peak from Si remains.[4]

between the various schemes is made on the basis of the degree of agreement between the actual spectral intensities and those required by the given model.

Figures 4 and 5 demonstrate the sensitivity of ESCA to the composition of the sample, but the Si(2p) spectra (Figure 6) reveal the shortcomings of the technique. While the Si(2p) binding energy shifts progressively with changes in the Si/Al ratio, the spectrum is insensitive to the *distribution* of Si(nAl) in the first tetrahedral shell, readily seen by ^{29}Si MAS NMR. This is reflected in the essentially constant Si(2p) line widths for the Na-A, Na-X, Na-Y sequence. The absence of line broadening for zeolite Na-X compared to the other two suggests that the symmetric tetrahedrally oriented charge fields are averaged even for the first shell.

Table 3 reveals other features of ESCA. Thus, the main reason the difference in the Si(2p) shift between zeolite
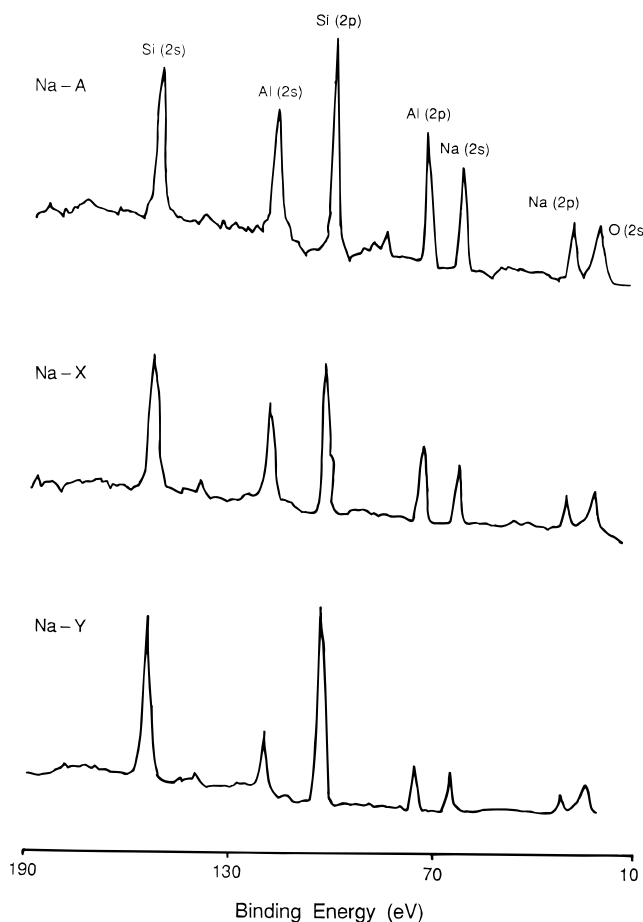
FIGURE 5. ESCA valence band spectra of zeolites Na-Y (Si/Al = 2.5), Na-X (Si/Al = 1.25), and Na-A (Si/Al = 1.0).
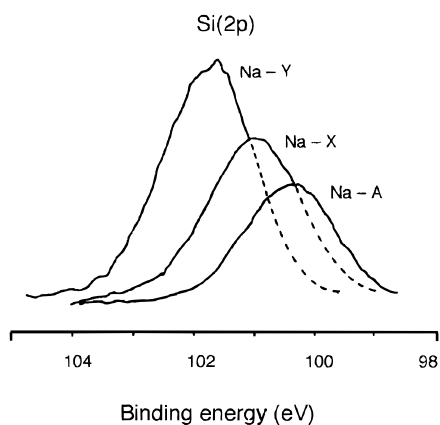

FIGURE 6. Si(2p) ESCA spectra of zeolites Na-Y (Si/Al = 2.5), Na-X (Si/Al = 1.25), and Na-A (Si/Al = 1.0).[4]

Table 3. Si(2p) ESCA Chemical Shifts of the Central Si Atom (in Bold Type) in Different Si(OAl)$_n$(OSi)$_{4-n}$ Structural Units

structural unit	Si(2p) shift (eV)	structural unit	Si(2p) shift (eV)
Si(OAl)$_4$	101.0	**Si**(OAl)(OSi)$_3$	102.6
Si(OAl)$_3$(OSi)	101.7	**Si**(OSi)$_4$	103.4
Si(OAl)$_2$(OSi)$_2$	102.2		

Na-A and pure silica is more than twice the size of the total range of Al(2p) shifts is the fact that the Si(2p) shifts are caused by the composition of the *first* tetrahedral

coordination shell of Si which can be of five different Si-(*n*Al) kinds, while the composition of the first coordination shell of Al is always Al(4Si), so that the Al(2p) shifts reflect the composition of the *second* coordination shell. The effect of the first shell is about twice that of the second.[4] Another reason for the different behavior of Si(2p) and Al(2p) ESCA shifts is the Q^C values in (6) which may be different.[13−15]

The correlation between the ^{29}Si chemical shift and the Si−O−Si bond angles and Si−O bond distances in silicates is useful for structural determination.[24−28] Several relationships have been proposed to quantify this effect,[5] supported by quantum-mechanical correlations between the chemical shift and the change of the *s* character of the oxygen orbitals in the Si−O−Si σ bond. These correlations, confirmed by an extended set of experimental data, are of assistance in spectral assignment, and allow the evolution of the structure during phase transformations to be monitored.[29]

Aluminum. ^{27}Al has a 100% natural abundance, with *I* = 5/2 and a chemical shift range of ca. 80 ppm in zeolites.[5] Chemical information can be obtained from ^{27}Al spectra provided quadrupole coupling and chemical shift effects can be separated. This is possible using MAS alone or in combination with other techniques.

The isotropic ^{27}Al NMR chemical shifts depend on the coordination of aluminum with respect to oxygen. Chemical shifts of 55−80 and 0−22 ppm from Al(H$_2$O)$_6$$^{3+}$ are observed in aluminosilicates for 4- and 6-coordinate Al, respectively. The width of both ranges indicates that the shift is influenced not only by the coordination, but also by the composition of the second coordination sphere and by the nature of the charge-balancing cation.

^{27}Al MAS NMR spectra of as-prepared zeolites contain a single resonance from 4-coordinate Al, because all Al atoms are in the Al(4Si) environment. On the other hand, while Si in zeolites is always 4-coordinate, in chemically treated materials Al can be 4-, 5-, or 6-coordinate. Because of the quadrupolar interaction, the line width of the ^{27}Al resonance is sensitive to the symmetry of the nuclear environment. ^{27}Al NMR can thus probe the coordination, quantity, and location of Al atoms, but is less useful than ^{29}Si NMR for direct structural determination.

Relationships similar to those for ^{29}Si chemical shifts hold between ^{27}Al NMR chemical shifts corrected for the quadrupole interaction and mean Al−O−Al bond angles.[30] However, since the total range of chemical shifts for 4-coordinate Al is only ca. 10 ppm and the isotropic ^{27}Al shifts are difficult to measure accurately, this relationship is of less practical value.

Figure 7 explains why ESCA spectra produce a progressive change in chemical shift for framework Al as the Si/Al ratio increases from 1 to 100, while the position and line width of the ^{27}Al NMR resonance remain virtually constant. The Al(4Si) environment for each Al atom defines the radial extent of the NMR chemical shifts, so that the ^{27}Al resonance is affected by the Si of the first tetrahedral shell, but the effect of the second shell (the composition of which may vary between 4Si and 4Al) is
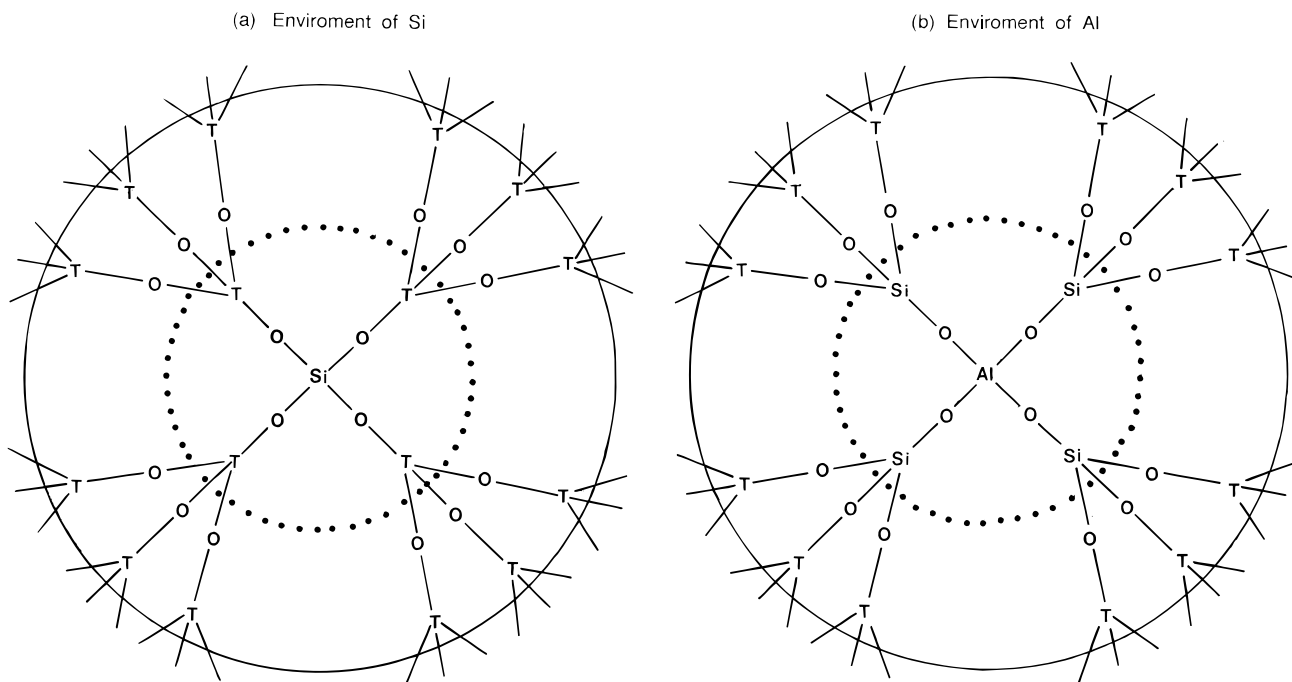
(a) Enviroment of Si

(b) Enviroment of Al

FIGURE 7. The environment of (a) silicon and (b) aluminum atoms in zeolites. T denotes either Si or Al, with the restriction that Al atoms cannot be linked via oxygens. Dashed and solid lines enclose the regions of sensitivity of NMR and ESCA, respectively. In NMR, the more localized and directional effects give a clear picture of immediate bonding, while ESCA is sensitive to the second coordination shell, but nondirectional.
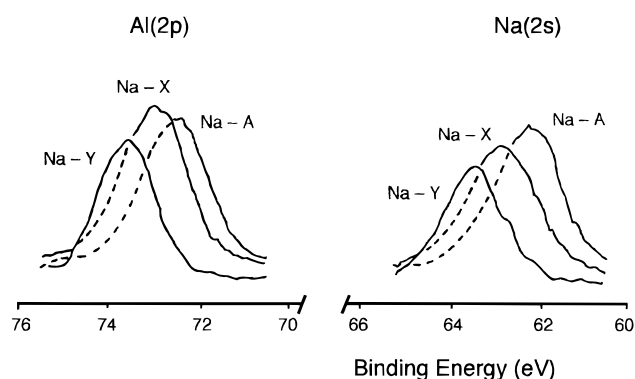
Al(2p)

Na(2s)

Binding Energy (eV)

FIGURE 8. Al(2p) and Na(2s) ESCA spectra of zeolites Na-Y (Si/Al = 2.5), Na-X (Si/Al = 1.25), and Na-A (Si/Al = 1.0).

much smaller. The ^{27}Al line from framework Al is therefore relatively symmetric. This also explains why the ^{29}Si NMR chemical shifts so closely replicate the tetrahedral Si(nAl) distribution in the first shell around a Si atom, irrespective of the composition of the second shell, the distance to which is greater than 10 Å.

Consider the Al(2p) ESCA binding energies (Figure 8) in terms of the model in Figure 7, where all Al atoms are surrounded by four Si atoms in the first shell and by either Si or Al in the second shell. If the range of influence of ESCA binding energies were as localized as it is for NMR, all zeolites would give the same symmetric Al(2p) peak irrespective of the Si/Al ratio. In fact, the increase of the Si/Al ratio does correspond to a progressive shift in Al(2p) binding energy (Table 2), although the effect is only half the size of that for Si(2p) with the same change in the Si/Al ratio. In view of Figure 7, it is clear that the Al(2p) shifts are caused by the variation in the average

Q^A charge field from the second and subsequent shells, showing that the ESCA chemical shifts are less localized than the NMR shifts for the same sample. This is because ESCA monitors binding energy changes induced by variations in electronic charge fields, while NMR registers the vector potential established by the interaction of electrons with the nuclear magnetic moment. Thus, ESCA not only can "see" much more clearly than NMR all the way to the second shell, but also responds to the alterations in the charge field of the oxygens and registers the changes in the state of oxygen between the first and the second shells.

A distinct advantage for NMR is apparent from these results. Although the Al(2p) peaks are shifted for zeolite Na-Y compared with Na-A,[2] ESCA does not readily respond to the different distributions of Al and Si in the second coordination shell around each Al corresponding to Si/Al = 2.5 in zeolite Na-Y. This averaging of the tetrahedral field is the ESCA equivalent of the "amalgamated bond" model[31] in optical spectroscopy. ESCA is thus relatively insensitive to structural features, something which is the main strength of NMR.[5]

Amorphous materials have no long-range *structural* order, but retain a long-range *chemical* order.[32] Thus, chemical bonds in SiO$_2$ glass are similar to those in crystalline SiO$_2$. ESCA, which monitors bonding over several tetrahedral shells, provides valuable information on glass chemistry, while NMR much more readily detects the difference between crystalline and glassy states.

Oxygen. ^{17}O has a wide range of chemical shifts[33] and a very low natural abundance and undergoes very large second-order quadrupole interactions (Table 1). The introduction of double-rotation (DOR) and dynamic-angle

spinning (DAS) NMR,[34−37] and of satellite transition spectroscopy,[38] enabled individual sites for oxygen in oxides to be resolved. DOR combined with isotopic enrichment resolves different oxygen sites in faujasite.[39] The 10° range of Si−O−Si angles was found to correspond to a 10.6 ppm change in the [17]O chemical shift. Multiple-quantum (MQ-MAS) NMR[40] promises further structural insights. The asymmetry parameter of the [17]O electric field gradient tensor is correlated with bond angles,[41] and MQ-MAS resolves two [17]O lines in the spectrum of zeolite ZSM-5, corresponding to the O(2Si) and O(Si,Al) environments. The relationship between bond angles and the [17]O chemical shift in silicates is likely to be similar to those for [29]Si and [27]Al.

While NMR is able to distinguish between the different distributions of Al atoms in aluminosilicates, ESCA is less specific because of its reliance on the average field generated by the various charges.[2] However, O(1s) ESCA spectra are readily available. The position of O(1s) ESCA core lines depends on the Si/Al ratio as strongly as the Si(2p) and Al(2p) lines.[4] The valence band spectra can be informative,[14] as the chemical behavior of oxides is reflected in the oxygen ESCA bands (Figure 5). Unfortunately, ESCA spectra of oxides are seldom reported.[1,17,19]

The O(1s) ESCA line shifts progressively in the spectra of many aluminosilicates as the Si/Al ratio changes.[1,2,15,17] The size of the total shift in zeolites is similar to that for the Si(2p) line. The O(1s) and Si(2p) shifts for each step in a progressive change in the Si/Al ratio for any group of framework aluminosilicates are also similar (Table 3).[4]

The fact that while each silicon is bonded to four oxygens, an oxygen is bonded to only two tetrahedral atoms, forming Si−O−Al or Si−O−Si units, is reflected in the ESCA spectra. Also, (8) shows that while effects associated with the second coordination layer contribute to the ESCA chemical shifts of oxygen, the O(1s) peak position is mainly controlled by the first term, which accounts for changes induced in the charge on the oxygen, Q^O, by the mixing of -Si−O−Si- and -Si−O−Al- units.[2] When either of the two compositional extremes is reached, only two situations are possible: -Si−O−Si- and -Si−O−Al-.[42] The intermediate Si/Al ratios should be reflected in the O(1s) spectra through the linear polarization of Q^O, and a mixture of the two spectra, rather than the average shift, should be observed.[13] Table 2 shows that, while the Al(2p), Si(2p), and O(1s) lines from zeolite Na-A and SiO_2 are narrow, in zeolite Na-Y (Si/Al = 2.5), which contains both types of linkages, the Al(2p) and Si(2p) lines are narrow, but the O(1s) line is broad. This is always the case in zeolites with intermediate Si/Al ratios. The effect is analogous to the broadening of the ^{29}Si NMR peaks in the spectra of zeolites containing a mixture of Si(3Al), Si(2Al), and Si(1Al) structural units. Broadening of the O(1s) peaks is also found in the spectra of zeolites containing multivalent cations.[2]

While NMR can quantify the various Si(*n*Al) environments, ESCA is incapable of this even at its highest resolution. However, very high-resolution ESCA may soon be able to monitor some of these effects.[2] The ESCA and

NMR spectra of ultramarine, an isomorph of sodalite, may seem exceptional (Table 2), but they simply reflect the fact that this pyrolytically prepared material violates the Loewenstein rule.[43]

References

(1) *Practical Surface Analysis*, 2nd ed.; Briggs, D., Seah, M. P., Eds.; John Wiley: Chichester, U.K., 1990.
(2) Barr, T. L. *Modern ESCA: The Principles and Practice of X-ray Photoelectron Spectroscopy*; CRC Press: Boca Raton, FL, 1994; Chapter 8.
(3) Lambert, S. L.; Lawson, R. J.; Johnson, R. W.; Barr, T. L. Catalytic Composite for Conversion of Hydrocarbons and Their Method of Preparation. U.S. Patent No. 4,619,906, 1986.
(4) Barr, T. L. An ESCA study of of Si as it occurs in adsorbents, catalysts and thin films. *Appl. Surf. Sci.* **1983**, *15*, 1−35.
(5) Engelhardt, G.; Michel, D. *High-Resolution Solid-State NMR of Silicates and Zeolites*; John Wiley: Chichester, 1987.
(6) Siegbahn, K.; Nordling, C.; Johansson, G.; Hedman, J.; Hedén, P. F.; Hamrin, K.; Gelius, U.; Bergmark, T.; Werme, L. O.; Manne, R.; Baer, Y. *ESCA Applied to Free Molecules*; North-Holland: Amsterdam, 1969.
(7) Davis, D. W.; Shirley, D. A. Prediction of core-level binding energy shifts from CNDO molecular orbitals. *J. Electron Spectrosc. Relat. Phenom.* **1974**, *3*, 137.
(8) Barr, T. L.; Seal, S.; Wozniak, K.; Klinowski, J. ESCA studies of the coordination state of aluminium in oxide environments. *J. Chem. Soc., Faraday Trans.* **1997**, *93*, 181−186.
(9) Minachev, K. M.; Shpiro, E. S. *Catalyst Surface: Physical Methods of Studying*; CRC Press: Boca Raton, FL, 1990.
(10) He, H. Y.; Alberti, K.; Barr, T. L.; Klinowski, J. ESCA studies of aluminophosphate molecular sieves. *J. Phys. Chem.* **1993**, *97*, 13703−13707.
(11) Herreros, B.; He, H. Y.; Barr, T. L.; Klinowski, J. ESCA studies of framework silicates with the sodalite structure. 1. Comparison of purely siliceous sodalite and aluminosilicate sodalite. *J. Phys. Chem.* **1994**, *98*, 1302−1305.
(12) Barr, T. L. Correlation of ESCA binding energy shifts with changes in zeolite structure and cations. *ACS, Div. Pet. Chem.* **1978**, *23*, 82.
(13) Barr, T. L.; Lishka, M. A. ESCA studies of the surface chemistry of zeolites. *J. Am. Chem. Soc.* **1986**, *108*, 3178−3186.
(14) Barr, T. L.; Li, M. C.; Mohsenian, M.; Lishka, M. A. XPS valence band study of zeolites and related systems. 1. General chemistry and structure. *J. Am. Chem. Soc.* **1988**, *110*, 7962−7975.
(15) Barr, T. L. The nature of the relative bonding chemistry in zeolites: an XPS study. *Zeolites* **1990**, *10*, 760−765.
(16) Wagner, C. D.; Six, H. A.; Jensen, W. T.; Taylor, J. A. Improving the accuracy of determination of line energies by ESCA: Chemical state plots for silicon aluminum compounds. *Appl. Surf. Sci.* **1981**, *9*, 203−213.
(17) Barr, T. L. Advances in the application of X-ray photoelectron spectroscopy (ESCA). 2. New methods. *Crit. Rev. Anal. Chem.* **1991**, *22*, 229−325.
(18) Barr, T. L. Recent advances in X-ray photoelectron spectroscopy studies of oxides. *J. Vacuum Sci. Technol.* **1991**, *A9*, 1793−1805.

(19) Barr, T. L. Advances in the application of X-ray photoelectron spectroscopy (ESCA). 1. Foundation and established methods. *Crit. Rev. Anal. Chem.* **1991**, *22*, 115−181.

(20) Engelhardt, G.; Lohse, U.; Lippmaa, E.; Tarmak, M.; Mägi, M. Si-29 NMR investigation of silicon−aluminum ordering in the aluminosilicate framework of faujasite-type zeolites. *Z. Anorg. Allg. Chem.* **1981**, *482*, 49−64.

(21) Loewenstein, W. The distribution of aluminum in the tetrahedra of silicates and aluminates. *Am. Mineral.* **1954**, *39*, 92−96.

(22) Klinowski, J.; Ramdas, S.; Thomas, J. M.; Fyfe, C. A.; Hartman, J. S. A reexamination of Si,Al ordering in zeolites NaX and NaY. *J. Chem. Soc., Faraday Trans. 2* **1982**, *78*, 1025−1050.

(23) Melchior, M. T.; Vaughan, D. E. W.; Jacobson, A. J. Characterization of the silicon aluminum distribution in synthetic faujasites by high-resolution solid-state Si-29 NMR. *J. Am. Chem. Soc.* **1982**, *104*, 4859−4864.

(24) Smith, J. V.; Blackwell, C. S. Nuclear magnetic resonance of silica polymorphs. *Nature* **1983**, *303*, 223−225.

(25) Thomas, J. M.; Klinowski, J.; Ramdas, S.; Hunter, B. K.; Tennakoon, D. T. B. The evaluation of non-equivalent tetrahedral sites from ²⁹Si NMR chemical shifts in zeolites and related aluminosilicates. *Chem. Phys. Lett.* **1983**, *102*, 158−162.

(26) Ramdas, S.; Klinowski, J. A simple correlation between isotropic ²⁹Si NMR chemical shifts and T−O−T angles in zeolite frameworks. *Nature* **1984**, *308*, 521−523.

(27) Engelhardt, G.; Radeglia, R. A semi-empirical quantum-chemical rationalization of the correlation between Si−O−Si angles and Si-29 NMR chemical shifts of silica polymorphs and framework aluminosilicates (zeolites). *Chem. Phys. Lett.* **1984**, *108*, 271−274.

(28) Engelhardt, G.; Luger, S.; Buhl, C.; Felsche, J. Si-29 NMR spectroscopy of sodalites: correlations between chemical shift and structural parameters. *Z. Krist.* **1988**, *182*, 82−83.

(29) Liu, S. X.; Welch, M. D.; Klinowski, J. NMR study of phase transitions in guest-free silica clathrate melanophlogite. *J. Phys. Chem.* **1997**, *B101*, 2811−2814.

(30) Lippmaa, E.; Samoson, A.; Magi, M. High-resolution Al-27 NMR of aluminosilicates. *J. Am. Chem. Soc.* **1986**, *108*, 1730−1735.

(31) Onodera, Y.; Toyozawa, Y. Persistence and amalgamation types in the electronic structure of mixed crystals. *J. Phys. Soc. Jpn.* **1966**, *24*, 341−355.

(32) Fehlner, F. *Low Temperature Oxidation*; Wiley-Interscience: New York, 1986.

(33) Kitzinger, J. P. *Oxygen-17 and Silicon-29*; Springer-Verlag: New York, 1981; Vol. 17, pp 1−64.

(34) Chmelka, B. F.; Mueller, K. T.; Pines, A.; Stebbins, J.; Wu, Y.; Zwanziger, J. W. Oxygen-17 NMR in solids by dynamic-angle spinning and double rotation. *Nature* **1989**, *339*, 42−43.

(35) Mueller, K. T.; Wu, Y.; Chmelka, B. F.; Stebbins, J.; Pines, A. High-resolution O-17 NMR of solid silicates. *J. Am. Chem. Soc.* **1991**, *113*, 32−38.

(36) Mueller, K. T.; Baltisberger, J. H.; Wooten, E. W.; Pines, A. Isotropic chemical shifts and quadrupolar parameters for O-17 using dynamic-angle spinning NMR. *J. Phys. Chem.* **1992**, *96*, 7001−7004.

(37) Grandinetti, P. J.; Baltisberger, J. H.; Farnan, I.; Stebbins, J. F.; Werner, U.; Pines, A. Solid-state O-17 magic-angle and dynamic-angle spinning NMR study of the SiO_2 polymorph coesite. *J. Phys. Chem.* **1995**, *99*, 12341−12348.

(38) Jäger, C.; Dupree, R.; Kohn, S. C.; Mortuza, M. G. O-17 satellite transition spectroscopy of amorphous SiO_2. *J. Non-Cryst. Solids* **1993**, *155*, 95−98.

(39) Bull, L. M.; Cheetham, A. K. O-17 NMR studies of siliceous faujasite. *Stud. Surf. Sci. Catal.* **1997**, *105*, 471−477.

(40) Frydman, L.; Harwood, J. S. Isotropic spectra of half-integer quadrupolar spins from bidimensional magic-angle-spinning NMR. *J. Am. Chem. Soc.* **1995**, *117*, 5367−5368.

(41) Sternberg, U. The bond angle dependence of the asymmetry parameter of the O-17 electric field gradient tensor. *Solid State NMR* **1993**, *2*, 181−190.

(42) van Bekkum, H.; Flanigen, E. M.; Jansen, J. C. *Introduction to Zeolite Science and Practice*; Elsevier: Amsterdam, 1991.

(43) Klinowski, J.; Carr, S. W.; Tarling, S. E.; Barnes, P. Magic-angle-spinning NMR shows the aluminosilicate framework of ultramarine to be disordered. *Nature* **1987**, *330*, 56−58.

AR9800486